Detection Probability of a CFAR Matched Filter with Signal Steering Vector Errors

Jun Liu, *Member, IEEE*, Weijian Liu, *Member, IEEE*, Bo Chen, *Member, IEEE*, Hongwei Liu, *Member, IEEE*, and Hongbin Li, *Senior Member, IEEE*

***Abstract*—Our aim in this work is to analyze the detection performance of a constant false alarm rata matched filter (CFAR-MF) which was developed for the detection problem in white Gaussian noise with unknown noise power. An exact expression for the detection probability of the CFAR-MF is derived in the mismatched case where mismatch exists between the actual signal steering vector and the nominal one. This theoretical expression can be used to facilitate the performance evaluation of the CFAR-MF in real-world scenarios when signal mismatch cannot be neglected.**

***Index Terms*—Constant false alarm rate, matched filter, signal detection, steering vector mismatch.**

I. Introduction

DETECTING a signal of interest (SOI) in additive white Gaussian noise (AWGN) is a common problem in radar, sonar and communications. When the noise power level is exactly known, a matched filter (MF) can be employed for the target detection [1, ch. 4]. In the MF, a vector (including the filter coefficients) aligned with the signal steering vector is used to integrate the target signal energy for achieving optimal performance. It is worth noting that the detection threshold of the MF for a given probability of false alarm is set by using the perfect knowledge of the noise power level. In practice, the noise power level is usually unknown, e.g., due to the variation of noise power as a function of weather, operating frequency, and duration time [2]. As a result, we have to use the estimated noise power level to replace the actual one in the threshold setting of the MF. Nevertheless, there often exists an error in the noise power estimate [3]–[6], and the uncertainty in the noise power level is usually, under normal operating conditions, within 2 dB [7]. Such uncertainty would result in a significant performance degradation for the MF.

To handle this issue caused by the noise uncertainty, a constant false alarm rate MF (CFAR-MF) was proposed in [1, ch. 4] without requiring prior knowledge of the noise power level. A complex version of the CFAR-MF was derived in [8, eq. (11)], where it is referred to as generalized energy detector. Finite-sum expressions for the probabilities of false alarm and detection of the CFAR-MF were obtained in [9]. It is shown that the probability of false alarm of the CFAR-MF is irrelevant to the noise power, and hence the CFAR-MF exhibits a constant false alarm rate (CFAR) property with respect to the noise power level.

It should be emphasized that the signal steering vector is assumed to be known perfectly in the studies mentioned above. However, in many realistic applications, the actual signal steering vector is not always aligned with the presumed one [10]–[16]. For example, mismatch in the steering vector often exists in an array system, due to errors in calibration or look direction, distortions in signal waveform or array geometry. Obviously, the mismatch in the signal steering vector would lead to a performance loss for the CFAR-MF.

To the best of our knowledge, the detection performance of the CFAR-MF has not been studied in the presence of signal steering vector mismatch. In this study, we derive a closed-form expression for the detection probability of the CFAR-MF in the mismatched case where the actual signal steering vector is misaligned with the nominal one. This theoretical expression is verified by Monte Carlo (MC) simulations. In practice, we can use this theoretical expression to facilitate the performance evaluation of the CFAR-MF in the mismatched case.

Notation: Vectors (matrices) are denoted by boldface lower (upper) case letters. Superscripts $(\cdot)^T$, $(\cdot)^*$ and $(\cdot)^\dagger$ denote transpose, complex conjugate and complex conjugate transpose, respectively. $\mathrm{C}_m^n = \frac{m!}{n!(m-n)!}$ is the binomial coefficient. $\mathbf{I}$ stands for an identity matrix, and $\Gamma(\cdot)$ is the Gamma function defined as $\Gamma(n) = \int_0^\infty x^{n-1}\mathrm{e}^{-x}\mathrm{d}x$. $|\cdot|$ represents the modulus of a complex number, $||\cdot||$ denotes the Frobenius norm of a vector, and $\jmath = \sqrt{-1}$. $\mathcal{CN}$ stands for a circularly symmetric, complex Gaussian distribution. χ_n^2 denotes a central real Chi-squared distribution with degrees of freedom n, and $\chi_n'^2(\zeta)$ denotes a noncentral real Chi-squared distribution with degrees of freedom n and noncentrality parameter ζ.

Manuscript received September 18, 2015; revised October 19, 2015; accepted October 20, 2015. Date of publication October 26, 2015; date of current version October 29, 2015. This work was supported by the National Natural Science Foundation of China under Contracts 61501351, 61501505, and 61372132, the Program for Young Thousand Talent by Chinese Central Government , the Program for New Century Excellent Talents in University under Grant NCET-13-0945, and by the Fundamental Research Funds for the Central Universities under Grant XJS14039. The associate editor coordinating the review of this manuscript and approving it for publication was Prof. Bruno Demissie.

J. Liu, C. Bo, and H. Liu are with the National Laboratory of Radar Signal Processing, Xidian University, Xi'an 710071, China, and also with the Collaborative Innovation Center of Information Sensing and Understanding at Xidian University (e-mail: junliu@xidian.edu.cn; bchen@mail.xidian.edu.cn; hwliu@xidian.edu.cn).

W. Liu is with Wuhan Radar Academy, Wuhan 430019, China (e-mail: liuvjian@163.com).

H. Li is with the Department of Electrical and Computer Engineering, Stevens Institute of Technology, Hoboken, NJ 07030 USA (e-mail: hongbin.li@stevens.edu).

Color versions of one or more of the figures in this paper are available online at http://ieeexplore.ieee.org.

Digital Object Identifier 10.1109/LSP.2015.2494013

II. Problem Formulation

In the detection problem we take into consideration, the received N-dimensional data $\mathbf{x}$ is constrained to be of the form

$$\mathbf{x} = \mathbf{s}a + \mathbf{n}, \tag{1}$$

where $\mathbf{s} \in \mathbb{C}^{N\times 1}$ is a signal steering vector; a is a deterministic but unknown complex scalar accounting for the target reflectivity and channel propagation effects; $\mathbf{n}$ is a noise data vector and is assumed to have a complex circular Gaussian distribution with zero mean and covariance matrix $\sigma^2\mathbf{I}$, i.e., $\mathbf{n} \sim \mathcal{CN}(\mathbf{0}, \sigma^2\mathbf{I})$, where σ^2 is the noise power. Notice that if the noise covariance matrix is originally $\sigma^2\mathbf{R}$ where $\mathbf{R}$ is a known and positive definite matrix, we can use $\mathbf{R}^{-1/2}$ to whiten the received data, and then obtain the data model (1). This data model is often used in spatial and/or temporal signal processing.

The decision on the signal presence can be formulated into a hypothesis test that distinguishes between the noise-only hypothesis (H_0) and the signal-plus-noise hypothesis (H_1), namely,

$$\begin{cases} H_0 : \mathbf{x} \sim \mathcal{CN}(\mathbf{0}, \sigma^2\mathbf{I}), \\ H_1 : \mathbf{x} \sim \mathcal{CN}(\mathbf{s}a, \sigma^2\mathbf{I}). \end{cases} \tag{2}$$

A. Prior Work

As derived in [8, eq. (11)], a generalized likelihood ratio test solution to the detection problem in the case of unknown noise power can be derived as

$$\Xi = \frac{\mathbf{x}^\dagger \mathbf{P_s x}}{\mathbf{x}^\dagger \mathbf{P_s^\perp x}} \underset{H_0}{\overset{H_1}{\gtrless}} \xi, \tag{3}$$

where ξ is a detection threshold,

$$\mathbf{P_s} = \mathbf{s}(\mathbf{s}^\dagger\mathbf{s})^{-1}\mathbf{s}^\dagger, \text{ and } \mathbf{P_s^\perp} = \mathbf{I} - \mathbf{P_s}. \tag{4}$$

As obtained in [9], the probability of false alarm is

$$P_{\text{FA}} = (1+\xi)^{-(N-1)}, \tag{5}$$

and the detection probability is

$$P_{\text{D}} = 1 - (1+\xi)^{-(N-1)} \exp\left(-\frac{\beta}{1+\xi}\right) \times \sum_{j=1}^{N-1} \mathrm{C}_{N-1}^{j} \xi^j \sum_{m=0}^{j-1} \frac{1}{m!}\left(\frac{\beta}{1+\xi}\right)^m, \tag{6}$$

where

$$\beta = \frac{\|\mathbf{s}a\|^2}{\sigma^2}. \tag{7}$$

B. CFAR Matched Filter in Mismatched Case

The above results are obtained on the assumption that the actual steering vector $\mathbf{s}$ is exactly known. In practice, there may exist mismatch between the actual steering vector $\mathbf{s}$ and the nominal steering vector $\tilde{\mathbf{s}}$, i.e., $\mathbf{s} \neq \tilde{\mathbf{s}}$. In such a case, a detector can be obtained by replacing $\mathbf{s}$ with $\tilde{\mathbf{s}}$ in (3), i.e.,

$$\Lambda = \frac{\mathbf{x}^\dagger \mathbf{P}_{\tilde{\mathbf{s}}} \mathbf{x}}{\mathbf{x}^\dagger \mathbf{P}_{\tilde{\mathbf{s}}}^\perp \mathbf{x}} \underset{H_0}{\overset{H_1}{\gtrless}} \lambda, \tag{8}$$

where λ is a detection threshold,

$$\mathbf{P}_{\tilde{\mathbf{s}}} = \tilde{\mathbf{s}}(\tilde{\mathbf{s}}^\dagger\tilde{\mathbf{s}})^{-1}\tilde{\mathbf{s}}^\dagger, \text{ and } \mathbf{P}_{\tilde{\mathbf{s}}}^\perp = \mathbf{I} - \mathbf{P}_{\tilde{\mathbf{s}}}. \tag{9}$$

The mismatch between the actually and nominal steering vectors is described by

$$\cos^2\phi = \frac{|\mathbf{s}^\dagger\tilde{\mathbf{s}}|^2}{\|\mathbf{s}\|^2\|\tilde{\mathbf{s}}\|^2}. \tag{10}$$

Note that the amount of mismatch increases as $\cos^2\phi$ decreases.

The signal steering vector mismatch does not affect the probability of false alarm, since the received data include no target signal under H_0. Therefore, the probability of false alarm of the detector (8) is (5) with ξ replaced by λ. It can be seen from (5) that the detector (8) exhibits a CFAR property with respect to the noise power. Hence, we refer to the detector (8) as a CFAR-MF.

It is worth noting that the signal steering vector mismatch would have an obvious influence on the detection probability, and the expression (6) for the detection probability is invalid for the CFAR-MF in (8). In the following, we derive an exact expression for the detection probability of the CFAR-MF in the mismatched case.

III. Detection Probability in the Mismatched Case

Define

$$t = \frac{2}{\sigma^2}\mathbf{x}^\dagger\mathbf{P}_{\tilde{\mathbf{s}}}\mathbf{x}, \text{ and } \tau = \frac{2}{\sigma^2}\mathbf{x}^\dagger\mathbf{P}_{\tilde{\mathbf{s}}}^\perp\mathbf{x}. \tag{11}$$

The CFAR-MF in (8) can be rewritten as

$$\Lambda = \frac{t}{\tau} \underset{H_0}{\overset{H_1}{\gtrless}} \lambda. \tag{12}$$

It is easy to show that under H_1,

$$\begin{cases} t \sim \chi_2'^2(2\delta_1), \\ \tau \sim \chi_{2(N-1)}'^2(2\delta_2), \end{cases} \tag{13}$$

where

$$\begin{cases} \delta_1 = \frac{1}{\sigma^2}|\mathbf{P}_{\tilde{\mathbf{s}}}\mathbf{s}a|^2, \\ \delta_2 = \frac{1}{\sigma^2}|\mathbf{P}_{\tilde{\mathbf{s}}}^\perp\mathbf{s}a|^2. \end{cases} \tag{14}$$

Using (7) and (10), we can write (14) as

$$\begin{cases} \delta_1 = \beta\cos^2\phi, \\ \delta_2 = \beta(1-\cos^2\phi). \end{cases} \tag{15}$$

The probability density function of τ under H_1 is [17, eq. (29.4)]

$$f(\tau; 2(N-1), 2\delta_2) = \frac{1}{2}\mathrm{e}^{-\frac{\tau}{2}-\delta_2}\left(\frac{\tau}{2\delta_2}\right)^{\frac{N-2}{2}} I_{N-2}\left(\sqrt{2\tau\delta_2}\right), \tag{16}$$

where $I_n(\cdot)$ is the modified Bessel function of the first kind of order n. From [17, eq. (29.2)], we can obtain that the cumulative distribution function (CDF) of t under H_1 is

$$F(t; 2, 2\delta_1) = \Pr\left[\chi_2'^2(2\delta_1) \le t\right] = \sum_{n=0}^{\infty} \frac{\delta_1^n \mathrm{e}^{-\delta_1}}{2^{1+n} n! n!} \underbrace{\int_0^t y^n \mathrm{e}^{-y/2}\mathrm{d}y}_{\triangleq W(t)}. \tag{17}$$

According to [18, eq. 3.351.1], we have

$$W(t) = 2^{n+1} n! \left[1 - \mathrm{e}^{-\frac{t}{2}} \sum_{k=0}^{n} \frac{1}{k!} \left(\frac{t}{2} \right)^k \right]. \tag{18}$$

Plugging (18) into (17) yields

$$\begin{aligned} F(t; 2, 2\delta_1) &= \sum_{n=0}^{\infty} \frac{\delta_1^n \mathrm{e}^{-\delta_1}}{n!} \left[1 - \mathrm{e}^{-\frac{t}{2}} \sum_{k=0}^{n} \frac{1}{k!} \left(\frac{t}{2} \right)^k \right] \\ &= 1 - \mathrm{e}^{-\delta_1 - \frac{t}{2}} \sum_{n=0}^{\infty} \frac{\delta_1^n}{n!} \sum_{k=0}^{n} \frac{1}{k!} \left(\frac{t}{2} \right)^k, \end{aligned} \tag{19}$$

where we have used the equality $\sum_{n=0}^{\infty} \frac{\delta_1^n}{n!} = \mathrm{e}^{\delta_1}$. Further, the complementary CDF (tail distribution) of t under H_1 is

$$\begin{aligned} G(t; 2, 2\delta_1) &= \Pr \left[\chi_2'^2(2\delta_1) \geq t \right] \\ &= 1 - F(t; 2, 2\delta_1) \\ &= \mathrm{e}^{-\delta_1 - \frac{t}{2}} \sum_{n=0}^{\infty} \frac{\delta_1^n}{n!} \sum_{k=0}^{n} \frac{1}{k!} \left(\frac{t}{2} \right)^k. \end{aligned} \tag{20}$$

Before proceeding, we introduce an integral formula as follows:

$$\begin{aligned} &\int_0^{\infty} z^{\frac{n-1}{2}+i} \mathrm{e}^{-z} I_{n-1} \left(\sqrt{2\alpha z} \right) \mathrm{d}z \\ &= 2^{-\frac{n-1}{2}} i! \alpha^{\frac{n-1}{2}} \mathrm{e}^{\frac{\alpha}{2}} \sum_{j=0}^{i} \mathrm{C}_{i+n-1}^{i-j} \frac{1}{j!} \left(\frac{\alpha}{2} \right)^j. \end{aligned} \tag{21}$$

The derivation of (21) is given in Appendix A.

From (12), we can obtain the detection probability of the CFAR-MF in the mismatched case as

$$\begin{aligned} P_{\mathrm{D}} &= \int_0^{\infty} G(\tau\lambda; 2, 2\delta_1) f(\tau; 2(N-1), 2\delta_2) \mathrm{d}\tau \\ &= \mathrm{e}^{-(\delta_1+\delta_2)} \sum_{n=0}^{\infty} \frac{\delta_1^n}{n!} \sum_{k=0}^{n} \frac{\lambda^k}{\delta_2^{\frac{N-2}{2}} 2^{\frac{N}{2}+k} k!} h_k(\delta_2), \end{aligned} \tag{22}$$

where

$$h_k(\delta_2) \triangleq \int_0^{\infty} \tau^{k+\frac{N-2}{2}} \mathrm{e}^{-\frac{1+\lambda}{2}\tau} I_{N-2}(\sqrt{2\delta_2 \tau}) \mathrm{d}\tau. \tag{23}$$

Define $z = \frac{1+\lambda}{2}\tau$. Then, we can rewrite $h_k(\delta_2)$ as

$$\begin{aligned} &h_k(\delta_2) \\ &= \left(\frac{2}{1+\lambda} \right)^{k+\frac{N}{2}} \int_0^{\infty} z^{k+\frac{N-2}{2}} \mathrm{e}^{-z} I_{N-2} \left(\sqrt{\frac{4\delta_2}{1+\lambda} z} \right) \mathrm{d}z \\ &= (1+\lambda)^{-(k+N-1)} 2^{k+\frac{N}{2}} k! \delta_2^{\frac{N-2}{2}} \mathrm{e}^{\frac{\delta_2}{1+\lambda}} \\ &\quad \times \sum_{j=0}^{k} \mathrm{C}_{k+N-2}^{k-j} \frac{1}{j!} \left(\frac{\delta_2}{1+\lambda} \right)^j, \end{aligned} \tag{24}$$

where the second equality is obtained by using (21). Applying (24) to (22) leads to

$$\begin{aligned} P_{\mathrm{D}} &= \mathrm{e}^{-\delta_1 - \left(1 - \frac{1}{1+\lambda}\right)\delta_2} (1+\lambda)^{-(N-1)} \\ &\quad \times \sum_{n=0}^{\infty} \frac{\delta_1^n}{n!} \sum_{k=0}^{n} \left(\frac{\lambda}{1+\lambda} \right)^k \sum_{j=0}^{k} \mathrm{C}_{k+N-2}^{k-j} \frac{1}{j!} \left(\frac{\delta_2}{1+\lambda} \right)^j. \end{aligned} \tag{25}$$

It can be seen that the detection performance of the CFAR-MF is affected by the signal steering vector mismatch through the noncentrality parameters δ_1 and δ_2.

IV. Numerical Results

In this section, numerical simulations are conducted to check the validity of the above theoretical result. Assume that a radar system transmitting N coherent pulses is used. Here, we select $N = 8$. The normalized Doppler frequency of the target is assumed to be 0.1, namely, the actual signal steering vector is

$$\mathbf{s} = \frac{1}{\sqrt{N}} [1, \exp(\jmath 2\pi 0.1), \cdots, \exp(\jmath 2\pi (N-1) 0.1)]^T. \tag{26}$$

The signal-to-noise ratio (SNR) in decibel is defined as SNR $= 10 \log_{10} |a|^2/\sigma^2$.

Note that (25) is an infinite sum expression which is inconvenient for numerical calculation of the detection probability. In practice, we can use the first finite terms to approximate the detection probability. Denote

$$\begin{aligned} &\tilde{P}_{\mathrm{D}}(M) \\ &= \mathrm{e}^{-\delta_1 - (1 - \frac{1}{1+\lambda})\delta_2} (1+\lambda)^{-(N-1)} \sum_{n=0}^{M} \frac{\delta_1^n}{n!} \sum_{k=0}^{n} \left(\frac{\lambda}{1+\lambda} \right)^k \\ &\quad \times \sum_{j=0}^{k} \mathrm{C}_{k+N-2}^{k-j} \frac{1}{j!} \left(\frac{\delta_2}{1+\lambda} \right)^j. \end{aligned} \tag{27}$$

Obviously, $\tilde{P}_{\mathrm{D}}(M)$ is obtained by replacing the notation ∞ in the first summation of (25) by M.

Fig. 1(a) shows relative errors defined as

$$\text{Relative Error} = \frac{\tilde{P}_{\mathrm{D}}(M+1) - \tilde{P}_{\mathrm{D}}(M)}{\tilde{P}_{\mathrm{D}}(M+1)}. \tag{28}$$

The probability of false alarm is $P_{\mathrm{FA}} = 0.01$, and the nominal Doppler frequency is selected to be 0.12 (different to the actual Doppler frequency 0.1), namely, the nominal signal steering vector is

$$\tilde{\mathbf{s}} = \frac{1}{\sqrt{N}} [1, \exp(\jmath 2\pi 0.12), \cdots, \exp(\jmath 2\pi (N-1) 0.12)]^T. \tag{29}$$

It implies that mismatch occurs between the actual and nominal steering vectors, i.e., $\mathbf{s} \neq \tilde{\mathbf{s}}$ and $\cos^2\phi = 0.9198$. It can be seen in Fig. 1(a) that as M increases, the relative error decreases.

Fig. 1(b) plots the curves of $\tilde{P}_{\mathrm{D}}(M)$ as a function of M. For comparison, we also provide the detection probability obtained by MC simulations. The numbers of independent trials used for simulating the probabilities of false alarm and detection are $100/P_{\mathrm{FA}}$ and 10 000, respectively. We can observe that $\tilde{P}_{\mathrm{D}}(M)$ approaches the MC result as M increases. Specifically, the number of terms (i.e., M) required in the chosen parameter setting is 30 (or 50) when the SNR is 12 (or 15) dB.

Now we comment on how to choose a proper value of M in the calculation of the detection probability. The results in Fig. 1 highlight that the approximate detection probability $\tilde{P}_{\mathrm{D}}(M)$ is very close to the true value when the relative error is less than 10^{-4}. As a rule of thumb, M is selected in practice when the relative error is less than 10^{-4}. Such a rule is adopted for the detection probability calculation in the following simulations.

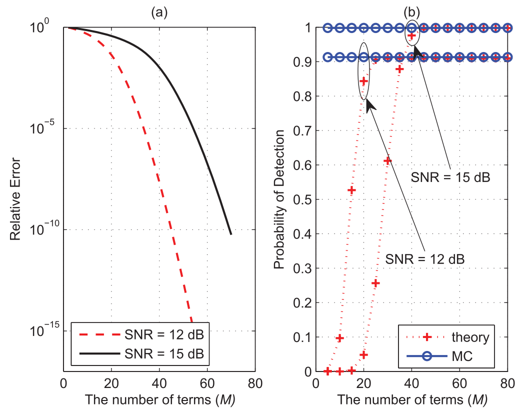

Fig. 1. Approximation errors.

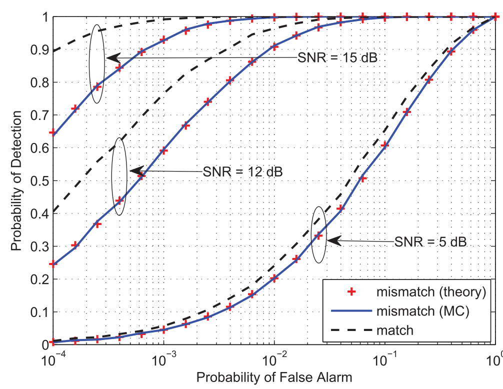

Fig. 2. ROC curves of the CFAR-MF.

In Fig. 2, we depict the receiver operating characteristic (ROC) curves of the CFAR-MF in both matched and mismatched cases where the parameters are the same as those in Fig. 1. It is illustrated in Fig. 2 that the theoretical results obtained with the first finite terms match the MC results pretty well. Additionally, the mismatch in the signal steering vector results in an obvious loss in the detection performance of the CFAR-MF.

Fig. 3 shows the detection performance of the CFAR-MF under different degrees of signal mismatch. It can be observed that the increase in the mismatch leads to the increase in performance loss. Note that in the region $\cos^2\phi \in [0.2, 0.4]$, the detection probability for SNR $= 15$ dB is slightly lower than that for SNR $= 12$ dB. This is because the mismatch may result in a leakage of the signal energy. As the SNR increases, the amount of the leaked signal energy may grow in the mismatched case, which leads to a decrease in the detection probability. Similar phenomena can be found in [13], [15], [19].

V. Conclusions

We have investigated the performance of the CFAR-MF which is designed for the detection problem in white Gaussian noise with unknown noise power. The exact expression for the detection probability of the CFAR-MF has been derived for the mismatched case where the nominal signal steering vector is misaligned with the actual one. Numerical examples show that the theoretical results match the MC results. This theoretical expression can serve as a mathematical tool for facilitating the performance evaluation of the CFAR-MF in practical applications when signal mismatch exists and cannot be neglected.

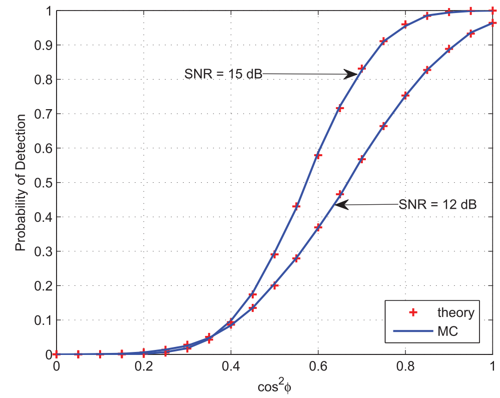

Fig. 3. Detection probability of the CFAR-MF with respect to $\cos^2\phi$.

Appendix

It is shown in [20, eq. (81)] that

$$Q_1 \triangleq \int_0^\infty x^{\mu-1} \mathrm{e}^{-p^2x^2} I_\nu(ax)\mathrm{d}x = \frac{\Gamma(\frac{\nu+\mu}{2})a^\nu}{2^{\nu+1}p^{\nu+\mu}\Gamma(\nu+1)} \mathrm{e}^{\frac{a^2}{4p^2}} {}_1F_1\left(\frac{\nu-\mu}{2}+1; \nu+1; -\frac{a^2}{4p^2}\right), \tag{30}$$

where ${}_1F_1(\cdot;\cdot;z)$ is the confluent hypergeometric function defined by

$${}_1F_1(m;n;z) = \sum_j^\infty \frac{(m)_j}{(n)_j}\frac{z^j}{j!} \tag{31}$$

with $(k)_j$ being the Pochhammer symbol [21]. Let $z = p^2x^2$ and $b = ap^{-1}$, then we have

$$Q_1 = \frac{1}{2p^\mu}\int_0^\infty z^{\frac{\mu-2}{2}} \mathrm{e}^{-z} I_\nu(b\sqrt{z})\mathrm{d}z. \tag{32}$$

From (30) and (32), we have

$$Q_2(\mu,\nu,b) \triangleq \int_0^\infty z^{\frac{\mu-2}{2}} \mathrm{e}^{-z} I_\nu(b\sqrt{z})\mathrm{d}z = \frac{\Gamma(\frac{\nu+\mu}{2})b^\nu}{2^\nu\Gamma(\nu+1)} \mathrm{e}^{\frac{b^2}{4}} {}_1F_1\left(\frac{\nu-\mu}{2}+1;\nu+1;-\frac{b^2}{4}\right). \tag{33}$$

Setting $\mu = n+2i+1$, $\nu = n-1$, and $b = \sqrt{2\alpha}$ in (33) yields

$$Q_2(n+2i+1, n-1, \sqrt{2\alpha}) = \int_0^\infty z^{\frac{n-1}{2}+i} \mathrm{e}^{-z} I_{n-1}(\sqrt{2\alpha z})\mathrm{d}z = \frac{\Gamma(n+i)\alpha^{\frac{n-1}{2}}}{2^{\frac{n-1}{2}}\Gamma(n)} \mathrm{e}^{\frac{\alpha}{2}} {}_1F_1\left(-i;n;-\frac{\alpha}{2}\right). \tag{34}$$

Using [22], we obtain

$${}_1F_1\left(-i;n;-\frac{\alpha}{2}\right) = \sum_{j=0}^i \frac{(-i)_j}{(n)_j}\frac{(-1)^j}{j!}\left(\frac{\alpha}{2}\right)^j = \sum_{j=0}^i \frac{\Gamma(i+1)\Gamma(n)}{\Gamma(i-j+1)\Gamma(n+j)j!}\left(\frac{\alpha}{2}\right)^j. \tag{35}$$

Substituting (35) into (34) results in (21).

REFERENCES

[1] L. L. Scharf, "Statistical signal processing: Detection," in *Estimation and Time Series Analysis*. Reading, MA, USA: Addison Wesley, 1991.

[2] M. S. Oude Alink, A. B. J. Kokkeler, E. A. M. Klumperink, G. J. M. Smit, and B. Nauta, "Lowering the SNR wall for energy detection using cross-correlation," *IEEE Trans. Veh. Technol.*, vol. 60, no. 8, pp. 3748–3757, Oct. 2011.

[3] A. Sonnenschein and P. M. Fishman, "Radiometric detection of spread-spectrum signals in noise of uncertain power," *IEEE Trans. Aerosp. Electron. Syst.*, vol. 28, no. 3, pp. 654–660, Jul. 1992.

[4] G. Ji and H. Zhu, "On the noise power uncertainty of the low SNR energy detection in cognitive radio," *J. Comput. Inf. Syst.*, vol. 6, no. 8, pp. 2457–2463, Jan. 2010.

[5] P. Wang, J. Fang, N. Han, and H. Li, "Multiantenna-assisted spectrum sensing for cognitive radio," *IEEE Trans. Veh. Technol.*, vol. 59, no. 4, pp. 1791–1800, May 2010.

[6] W. Yin, P. Ren, J. Cai, and Z. Su, "Performance of energy detector in the presence of noise uncertainty in cognitive radio networks," *Wireless Netw.*, vol. 19, no. 5, pp. 629–638, Jul. 2013.

[7] A. Kortun, T. Ratnarajah, M. Sellathurai, Y.-C. Liang, and Y. Zeng, "On the eigenvalue-based spectrum sensing and secondary user throughput," *IEEE Trans. Veh. Technol.*, vol. 63, no. 3, pp. 1480–1486, Mar. 2014.

[8] Y. Jin and B. Friedlander, "A CFAR adaptive subspace detector for second-order gaussian signals," *IEEE Trans. Signal Process.*, vol. 53, no. 3, pp. 871–884, Mar. 2005.

[9] J. Liu, Z.-J. Zhang, and Y. Yang, "Performance enhancement of subspace detection with a diversely polarized antenna," *IEEE Signal Process. Lett.*, vol. 19, no. 1, pp. 4–7, Jan. 2012.

[10] F. C. Robey, D. R. Fuhrmann, E. J. Kelly, and R. Nitzberg, "A CFAR adaptive matched filter detector," *IEEE Trans. Aerosp. Electron. Syst.*, vol. 28, no. 1, pp. 208–216, Jan. 1992.

[11] N. B. Pulsone and C. M. Rader, "Adaptive beamformer orthogonal rejection test," *IEEE Trans. Signal Process.*, vol. 49, no. 3, pp. 521–529, Mar. 2001.

[12] O. Besson, L. L. Scharf, and F. Vincent, "Matched direction detectors," in *Proc. IEEE Int. Conf. Acoustics, Speech, and Signal Processing*, Mar. 2005, pp. IV977–IV980.

[13] F. Bandiera, O. Besson, D. Orlando, and G. Ricci, "An ABORT-like detector with improved mismatched signals rejection capabilities," *IEEE Trans. Signal Process.*, vol. 56, no. 1, pp. 14–25, Jan. 2008.

[14] F. Bandiera, D. Orlando, and G. Ricci, *Advanced radar detection schemes under mismatched signal models*. San Rafael, CA, US: Morgan & Claypool, 2009.

[15] D. Orlando and G. Ricci, "A Rao test with enhanced selectivity properties in homogeneous scenarios," *IEEE Trans. Signal Process.*, vol. 58, no. 10, pp. 5385–5390, Oct. 2010.

[16] O. Besson and S. Bidon, "Robust adaptive beamforming using a bayesian steering vector error model," *Signal Process.*, vol. 93, no. 12, pp. 3290–3299, Dec. 2013.

[17] N. L. Johnson, S. Kotz, and N. Balakrishnan, *Continuous Univariate Distributions (Volumn 2)*, 2nd ed. New York, NY, USA: Wiley, 1995.

[18] I. S. Gradshteyn and I. M. Ryzhik, *Table of Integrals, Series, and Products*, 7th Ed. ed. San Diego, CA, USA: Academic, 2007.

[19] J. Liu, W. Liu, B. Chen, H. Liu, H. Li, and C. Hao, "Modified Rao test for multichannel adaptive signal detection," *IEEE Trans. Signal Process.*, DOI 10.1109/TSP.2015.2491892.

[20] W. Lindsey, "Error probabilities for rician fading multichannel reception of binary and N-ary signals," *IEEE Trans. Inf. Theory*, vol. IT-10, no. 4, pp. 339–350, Oct. 1964.

[21] "The wolfram function site: Pochhammer symbol," [Online]. Available: http://functions.wolfram.com/PDF/Pochhammer.pdf

[22] "The wolfram function site: Hypergeometric function," [Online]. Available: http://functions.wolfram.com/07.20.03.0116.01